Interactions of *Escherichia coli* Replicative Helicase PriA Protein with Single-Stranded DNA†

Maria J. Jezewska and Wlodzimierz Bujalowski*

Department of Human Biological Chemistry and Genetics, The University of Texas Medical Branch at Galveston, 301 University Boulevard, Galveston, Texas 77555-1053

Received May 16, 2000; Revised Manuscript Received June 26, 2000

ABSTRACT: Quantitative analyses of the interactions of the *Escherichia coli* replicative helicase PriA protein with a single-stranded DNA have been performed, using the thermodynamically rigorous fluorescence titration technique. The analysis of the PriA helicase interactions with nonfluorescent, unmodified nucleic acids has been performed, using the macromolecular competition titration (MCT) method. Thermodynamic studies of the PriA helicase binding to ssDNA oligomers, as well as competition studies, show that independently of the type of nucleic acid base, as well as the salt concentration, the type of salt in solution, and nucleotide cofactors, the PriA helicase binds the ssDNA as a monomer. The enzyme binds the ssDNA with significant affinity in the absence of any nucleotide cofactors. Moreover, the presence of AMP-PNP diminishes the intrinsic affinity of the PriA protein for the ssDNA by a factor ∼4, while ADP has no detectable effect. Analyses of the PriA interactions with different ssDNA oligomers, over a large range of nucleic acid concentrations, indicates that the enzyme has a single, strong ssDNA-binding site. The intrinsic affinities are salt-dependent. The formation of the helicase−ssDNA complexes is accompanied by a net release of 3−4 ions. The experiments have been performed with ssDNA oligomers encompassing the total site size of the helicase−ssDNA complex and with oligomers long enough to encompass only the ssDNA-binding site of the enzyme. The obtained results indicate that salt dependence of the intrinsic affinity results predominantly, if not exclusively, from the interactions of the ssDNA-binding site of the helicase with the nucleic acid. There is an anion effect on the studied interactions, which suggests that released ions originate from both the protein and the nucleic acid. Contrary to the intrinsic affinities, cooperative interactions between bound PriA molecules are accompanied by a net uptake of ∼3 ions. The PriA protein shows preferential intrinsic affinity for pyrimidine ssDNA oligomers. In our standard conditions (pH 7.0, 10 °C, 100 mM NaCl), the intrinsic binding constant for the pyrimidine oligomers is ∼1 order of magnitude higher than the intrinsic binding constant for the purine oligomers. The significance of these results for the mechanism of action of the PriA helicase is discussed.

Priming of the DNA strand during the replication process is catalyzed by a multiple protein complex, the primosome, which can translocate along DNA synthesizing short oligoribonucleotide primers that are used to initiate synthesis of the complementary strand (*1*−*3*). The PriA protein is a key replication protein in *Escherichia coli* that plays a fundamental role in the ordered assembly of the primosome (*1*−*3*). The protein was originally discovered to be an essential factor during the synthesis of the complementary DNA strand of phage ϕX174 DNA (*4*, *5*). Recent data indicate that the enzyme is involved not only in DNA replication but also in recombination and repair processes in the *E. coli* cell (ref *3* and references therein).

Studies in vitro demonstrate that the PriA protein displays multiple activities: (i) specific binding of ATPs and dATPs (*4*−*8*); (ii) ATPase and dATPase activities strongly stimulated by a specific DNA fragment, the primosome assembly site (PAS)[1] (*7*, *8*); (iii) specific strong binding to the PAS-DNA sequence (*7*−*9*); (iv) nonspecific binding to the ssDNA (*7*−*10*); (v) 3′ → 5′ helicase activity specifically stimulated by PAS (*11*, *12*). These multiple activities reflect complex interactions of the PriA protein with different ingredients in the primosome, replication fork, recombination, and repair complexes including protein−protein and protein−DNA interactions (*1*, *3*, *12*, *14*).

The gene encoding the PriA protein has been cloned and sequenced and that of the encoded protein has been determined (*13*, *14*). Current biochemical data suggest that the native protein is a monomer with a molecular mass of 81.7 kDa. The data also suggest that the monomer is the predominant form of the protein in solution (*7*−*9*).

In vivo functions of the PriA helicase are related to the ability of the protein to interact with both ss and dsDNA (*3*, *7*−*12*, *15*, *16*). Although the importance of understanding the PriA protein interactions with nucleic acid has been recognized, quantitative aspects of these interactions remain

† This work was supported by NIH Grants GM-46679 and GM-58675 (to W.B.).

* To whom correspondence should be addressed.

[1] Abbreviations: AMP-PNP, β,γ-imidoadenosine-5′-triphosphate; Tris, tris(hydroxymethyl)aminomethane; PAS, primosome assembly site; ATP, adenosine-5′-triphosphate; ADP adenosine-5′-diphosphate; DTT, dithiothreitol; EDTA, ethylenediaminetetraacetic acid disodium salt.

10.1021/bi001113y CCC: $19.00
Published on Web 07/29/2000

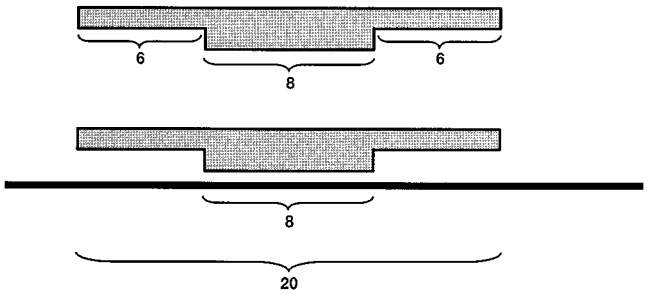

FIGURE 1: Schematic model of the PriA helicase−ssDNA complex. The ssDNA-binding site of the enzyme, which encompasses only eight nucleotide residues, is located in the center of the enzyme molecule. In the complex with the ssDNA (black ribbon), the enzyme occludes the total site size of 20 nucleotide residues with the protein matrix protruding over six residues on both sides of the ssDNA-binding site.

obscure. Particularly, little is known about the energetics of the protein−DNA complexes, effects of solution conditions, salt and type of salt on the intrinsic affinities and cooperativities, role of nucleotide cofactors, and base specificity in the PriA helicase−DNA complex formation.

Our recent studies indicate that the total site size of the PriA−ssDNA complex, i.e., the maximum number of nucleotide residues occluded by the PriA helicase in the complex, is $n = 20 \pm 3$ residues/protein monomer (Jezewska et al., *J. Biol. Chem.*, in press). However, the number of nucleotides directly engaged in interactions with the ssDNA-binding site of the helicase is only $m = 8 \pm 1$, i.e., it is significantly smaller than the total site size of the complex. Analysis of multiple stoichiometries of PriA complexes with ssDNA oligomers of different lengths indicates that the ssDNA-binding site is located in the central part of the enzyme molecule with the protein matrix protruding over a distance of ∼6 nucleotide residues on both sides of the ssDNA-binding site. Our current model of the PriA helicase−ssDNA complex is schematically depicted in Figure 1.

Knowledge of the energetics and mechanism of the helicase−nucleic acid complex and the mechanism of binding is of fundamental importance for our understanding of the enzyme functioning in DNA metabolism (*17*, *18*). This includes enzyme translocation on the DNA lattice, catalysis of the duplex DNA unwinding as well as the functioning of the PriA helicase in the formation and translocation of the primosome.

In this paper, we report the quantitative analyses of the PriA helicase interactions with the ssDNA. We present direct evidence that the PriA helicase binds the ssDNA as a monomer, independent of the type of the nucleic acid base, type of salt, and salt concentrations, as well as the presence of nucleotide cofactors. The formation of the helicase−ssDNA complexes is accompanied by a net ion release. Contrary to the intrinsic affinities, cooperative interactions between bound PriA molecules are accompanied by net ion uptake. While the presence of the ATP analogue diminishes the affinity of the PriA helicase for the ssDNA and affects the structure of the nucleic acid in the complex, ADP has very little effect on the intrinsic affinity and structure of the ssDNA in the complex with the helicase.

MATERIALS AND METHODS

Reagents and Buffers. All solutions were made with distilled and deionized >18 MΩ (Milli-Q Plus) water. All chemicals were reagent-grade. Buffer C is 10 mM sodium cacodylate adjusted to pH 7.0 with HCl, 0.1 mM EDTA, 1 mM DTT, and 25% glycerol. Selection of 25% glycerol in the buffer results from the fact that we have found that the stability of the PriA protein is significantly increased at higher glycerol concentrations. Temperatures and concentrations of salts in the buffer are indicated in the text.

PriA Protein. We isolated the gene of the *E. coli* PriA protein directly from the *E. coli* K12 strain. Sequencing of the isolated DNA revealed that the product of the PriA gene, isolated from the K12 strain, has an alanine residue in location 649; thus, it is identical to the PriA primary structure determined by Lee et al. (*14*). All experiments reported in this paper were performed with the product of the gene isolated by us from the K12 strain. We have also obtained the plasmid pET3c, harboring the gene of the PriA protein, from Dr. K. Marians (Sloan-Kettering), which has a valine residue in location 649 (*16*). Both proteins behave similarly in all thermodynamic tests reported in this work, indicating that the single amino acid difference in the sequence is not affecting interactions of the enzyme with the ssDNA. The isolated gene of the PriA helicase has been placed in pET30a plasmid (Novagen). With this system, we routinely obtain ∼800 mg of the pure enzyme from 100 g of cells. The enzyme used in our studies was >98% pure as judged by polyacrylamide electrophoresis with Coomassie Brilliant Blue staining. The concentration of the PriA protein was spectrophotometrically determined, with an extinction coefficient $\epsilon_{280} = 1.06 \times 10^5$ cm^{-1} M^{-1} (monomer) determined using an approach based on the Edelchoch method (*21*−*26*).

Nucleic Acids. Oligomers, dA(pA)$_9$, dA(pA)$_{17}$, dA(pA)$_{19}$, dA(pA)$_{25}$, dA(pA)$_{34}$, dC(pC)$_{19}$, and dT(pT)$_{19}$, were purchased from Midland Certified Reagents (Midland, Texas) and Sigma-Aldrich. Oligomers were at least >95% pure as judged by autoradiography on polyacrylamide gels. The etheno derivatives of adenosine oligomers were obtained by modification with chloroacetaldehyde (*19*, *27*). This modification goes to completion and provides a fluorescent derivative of the nucleic acid (*27*−*32*). The concentration of the etheno derivative of nucleic acids was determined using an extinction coefficient of 3700 cm^{-1} M^{-1} (Nucleotide) at 257 nm (*28*−*32*). The concentration of dC(pC)$_{19}$, dT(pT)$_{19}$, and dA(pA)$_{19}$ were determined using extinction coefficients (Nucleotide): $\epsilon_{270} = 7200$ cm^{-1} M^{-1}, $\epsilon_{260} = 8100$ cm^{-1} M^{-1}, and $\epsilon_{260} = 10\,000$ cm^{-1} M^{-1} (*28*−*32*).

Fluorescence Measurements. Steady-state fluorescence titrations were performed using SLM-AMINCO 48000S or 8100 spectrofluorometers. To avoid possible artifacts, due to the fluorescence anisotropy of the sample, polarizers were placed in excitation and emission channels and set at 90 and 55° (magic angle), respectively (*33*). The binding was followed by monitoring the fluorescence of the etheno derivative of the nucleic acids ($\lambda_{ex} = 325$ nm, $\lambda_{em} = 410$ nm). Computer fits were performed using KaleidaGraph software (Synergy Software, PA) and Mathematica (Wolfram Research, IL). The relative fluorescence increase of the nucleic acid, ΔF, upon binding the PriA protein is defined by

$$\Delta F = \frac{F_i - F_o}{F_o} \quad (1)$$

where F_i is the fluorescence of the nucleic acid solution at a given titration point "i", and F_o is the initial value of the fluorescence of the same solution.

Determination of Thermodynamically Rigorous Binding Isotherms of the PriA Helicase−ssDNA Complexes. In this work, we followed the binding of the PriA protein to ssDNA oligomers, by monitoring the fluorescence increase, ΔF_{obs}, of their etheno derivatives upon the complex formation. To obtain rigorous estimates of the average degree of binding, $\Sigma\Theta_i$ (number of bound protein molecules per ssDNA oligomer) and the free protein concentration, P_F, independent of any assumption about the relationship between the observed spectroscopic signal and $\Sigma\Theta_i$, we applied an approach previously described by us (*19*, *23*−*26*, *29*−*31*). Briefly, each different possible "i" complex of the PriA helicase with the ssDNA contributes to the experimentally observed fluorescence increase, ΔF_{obs}. Thus, ΔF_{obs} is functionally related to $\Sigma\Theta_i$ by

$$\Delta F_{obs} = \sum \Theta_i \Delta F_{imax} \qquad (2)$$

where ΔF_{imax} is the molecular parameter characterizing the maximum fluorescence increase of the nucleic acid with the PriA protein bound in complex "i". The same value of ΔF_{obs}, obtained at two different total nucleic acid concentrations, M_{T_1} and M_{T_2}, indicates the same physical state of the nucleic acid, i.e., the degree of binding, $\Sigma\Theta_i$, and the free PriA protein concentration, P_F, must be the same. The value of $\Sigma\Theta_i$ and P_F is then related to the total protein concentrations, P_{T_1} and P_{T_2}, and the total nucleic acid concentrations, M_{T_1} and M_{T_2}, at the same value of ΔF_{obs}, by

$$\sum \Theta_i = \frac{(P_{T_2} - P_{T_1})}{(M_{T_2} - M_{T_1})} \qquad (3a)$$

$$P_F = P_{T_X} - (\sum \Theta_i) M_{T_X} \qquad (3b)$$

where $x = 1$ or 2 (*19*, *28*−*32*, *34*, *35*).

Analysis of the PriA Binding to 10- and 18-mers of the ssDNA. A current model of the PriA helicase−ssDNA complex is schematically depicted in Figure 1. The total site size of the PriA helicase complex with the ssDNA is 20 ± 3 residues/protein monomer. However, the number of nucleotides, directly engaged in interactions with the ssDNA-binding site of the enzyme, is only $m = 8 \pm 1$ residues (Figure 1). Knowing the number of residues engaged in direct interactions with the ssDNA-binding site of the helicase allows us to properly extract the intrinsic binding constant, K_N, for ssDNA oligomers that bind only a single PriA molecule. Using K_N, the equation describing the binding of PriA to ssDNA oligomers, which can accommodate only a single enzyme molecule, is defined as

$$\Delta F = \Delta F_{max}\left[\frac{(N - m + 1)K_N P_F}{1 + (N - m + 1)K_N P_F}\right] \qquad (4)$$

where N is the number of nucleotide residues in the ssDNA oligomer, and ΔF_{max} is the maximum fluorescence increase accompanying the complex formation. It should be pointed out that the application of eq 4 assumes that the PriA protein must always engage eight nucleotide residues of the ssDNA in direct interactions.

Analysis of PriA Protein−Unmodified Nucleic Acid Complexes Using the MCT Method. Determination of the intrinsic affinities for the PriA helicase−unmodified nucleic acid complexes has been performed using the MCT method with the 18-mer, dϵA(pϵA)$_{17}$, as a reference fluorescent nucleic acid (*20*, *34*). Briefly, if the fluorescent reference nucleic acid at total concentration, M_{T_R}, is titrated with the protein in the presence of a competing nonfluorescent nucleic acid of total concentration, M_{1_S}, the total concentration of the protein, P_{T_1}, at which a given fluorescence change, ΔF_i, is observed is described by

$$P_{T_1} = (\sum \Theta_i)_S M_{1_S} + (\sum \Theta_i)_R M_{T_R} + P_F \qquad (5a)$$

where $(\Sigma\Theta_i)_R$, $(\Sigma\Theta_i)_s$, and P_F are the degree of binding of the protein on the reference fluorescent nucleic acid; the degree of binding of the protein on the nonfluorescent, competing oligomer; and the free protein concentration, respectively. The total concentration of the protein, P_{T_2}, at which the same ΔF_i is observed at the same M_{T_R}, but with a different total concentration of the competing nucleic acid, M_{2_S}, is described by

$$P_{T_2} = (\sum \Theta_i)_S M_{2_S} + (\sum \Theta_i)_R M_{T_R} + P_F \qquad (5b)$$

Subtracting eq 5a from eq 5b and rearranging provides eq 6, which allows us to determine the degree of binding of the protein on the competing, nonfluorescent ssDNA oligomer (*20*, *34*).

$$(\sum \Theta_i)_S = \frac{(P_{T_2} - P_{T_1})}{(M_{2_S} - M_{1_S})} \qquad (6)$$

Statistical Thermodynamic Model of PriA Helicase Binding to the 35-mer, dϵA(pϵA)$_{34}$. Our previous studies and the results described below show that the ssDNA 35-mer can accommodate two PriA molecules and the binding is accompanied by weak cooperative interactions. As we pointed out above, the protein engages in direct interactions with its ssDNA-binding site, only $m = 8$ nucleotide residues of the nucleic acid. This is much less than the total site size of the PriA−ssDNA complex ($n = 20 \pm 3$) (Figure 1). Therefore, binding of the first PriA molecule to dϵA(pϵA)$_{34}$ is described by an equation analogous to eq 4

$$\sum \Theta_i = \frac{(N - m + 1)K_{35} P_F}{1 + (N - m + 1)K_{35} P_F} \qquad (7)$$

where $N = 35$, $m = 8$, and K_{35} is the intrinsic binding constant for the 35-mer. Notice, a maximum of two PriA molecules can associate with the 35-mer. This allows us to apply combinatorial analysis for the binding of a large ligand to a finite lattice to derive a part of the partition function corresponding to the binding of two PriA molecules (*38*−*40*). The complete partition function of the PriA−dϵA(pϵA)$_{34}$

system, Z_{35}, is then

$$Z_{35} = 1 + (N - m + 1)K_{35}P_F + \sum_{j=0}^{k-1} S_N(k,j)(K_{35}P_F)^k\omega^j \quad (8)$$

where $k = 2$, and j is the number of cooperative contacts between the bound PriA molecules in a particular configuration on the lattice. The factor $S_N(k, j)$ is the number of distinct ways that two ligands bind to a lattice, with j cooperative contacts, and is defined by (*20*, *39*, *41*)

$$S_N(k,j) = \frac{[(N - (m+6)k + 1)!(k-1)!]}{[(N - (m+6)k - k + j + 1)!(k-j)!(k-j-1)!]} \quad (9)$$

The total degree of binding, $\Sigma\Theta_i$, is then defined as

$$\sum\Theta_i = \frac{[(N - m + 1)K_{35}P_F + \sum_{j=0}^{k-1} S_N(k,j)(K_{35}P_F)^k\omega^j]}{Z_{35}} \quad (10)$$

and the observed relative fluorescence increase of the nucleic acid is

$$\Delta F = \Delta F_1\left[\frac{(N - m + 1)K_{35}P_F}{Z_{35}}\right] + \Delta F_{max}\left[\frac{\sum_{j=0}^{k-1} S_N(k,j)(K_{35}P_F)^k\omega^j}{Z_{35}}\right] \quad (11)$$

where ΔF_1 and ΔF_{max} are relative molar fluorescence increases accompanying the binding of the one and two PriA molecules to the 35-mer.

RESULTS

Energetics within the Total Site Size of the PriA Helicase−ssDNA Complex. PriA Helicase−ssDNA 18-mer Interaction. We previously found that binding of the PriA helicase to etheno derivatives of the ssDNA is accompanied by a strong nucleic acid fluorescence increase (Jezewska et al., *J. Biol. Chem.*, in press). Such a large emission change provides an excellent signal to monitor the PriA−ssDNA interactions and to perform high-resolution measurements of the mechanism of the helicase−ssDNA complex formation and its structure (*36*, *37*). Quantitative analyses of the binding data showed that the total site size of the PriA−ssDNA complex, i.e., the maximum number of nucleotide residues occluded by the PriA helicase in the complex, is 20 ± 3 residues/protein monomer, as depicted in Figure 1. Thus, the total site size involves a minimum of 17 and a maximum of 23 nucleotide residues. To address the energetics of the helicase interactions with the ssDNA within the total site size of the formed complex, we selected the 18-mer, dϵA(pϵA)$_{17}$. This oligomer is within the total site size of the protein−nucleic acid complex and allows us to perform titrations in the large nucleic acid concentration range, avoiding the precipitation of the sample. A precipitation of the PriA−ssDNA complexes occurs at high protein and nucleic acid concentrations for longer oligomers and polymer ssDNAs (see below).

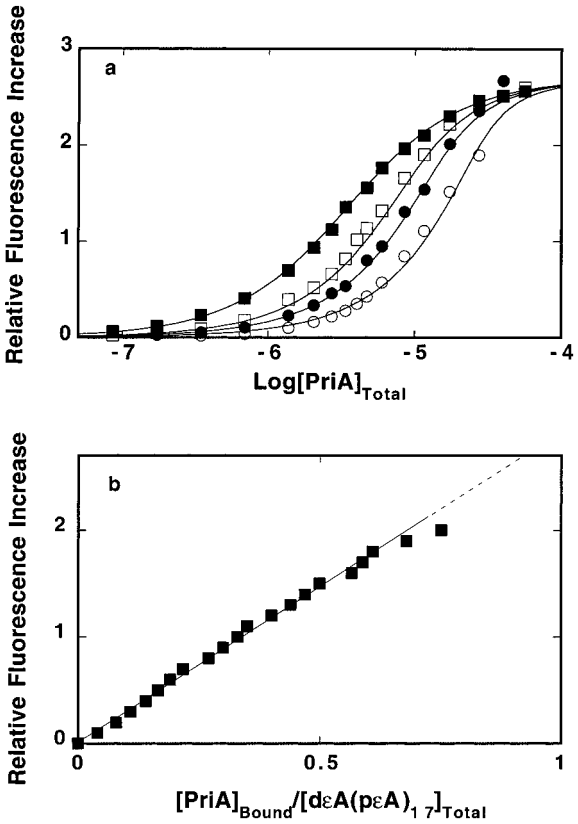

FIGURE 2: (a) Fluorescence titrations of the 18-mer, dϵA(pϵA)$_{17}$, with the PriA protein (λ_{ex} = 325 nm, λ_{em} = 410 nm) in buffer C (pH 7.0, 10 °C), containing 100 mM NaCl, at four different nucleic acid concentrations: (■) 1.42 × 10^{-6}, (□) 8.12 × 10^{-6}, (●) 1.35 × 10^{-5}, and (○) 2.71 × 10^{-5} M (oligomer). The solid lines are computer fits of the titration curves, using a single-site binding isotherm (eq 4) that takes into account the fact that the ssDNA-binding site engages only eight residues of the nucleic acid in direct interactions. Intrinsic binding constant K_1 = 3.3 × 10^4 M^{-1} and relative fluorescence change ΔF_{max} = 2.7. (b) Dependence of the relative fluorescence of the 18-mer, ΔF, upon the average number of bound PriA proteins (■). The solid line follows the experimental points and has no theoretical basis. The dashed line is the extrapolation of ΔF to the maximum value of ΔF_{max} = 2.7.

Fluorescence titrations of dϵA(pϵA)$_{17}$ with the PriA helicase, at four different nucleic acid concentrations, in buffer C (pH 7.0 10 °C), containing 100 mM NaCl, are shown in Figure 2a. As the nucleic acid concentration increases, a given relative fluorescence increase is reached at higher PriA protein concentrations. This results from the fact that at higher nucleic acid concentrations more protein is required to obtain the same degree of binding, $\Sigma\Theta_i$. A plateau of the titration curve at the highest 18-mer concentration could not be achieved because of the precipitation of the protein−nucleic acid complex at high protein and nucleic acid concentrations. Only the part of the curve where the precipitation is not evident is included. The selected nucleic acid concentrations provide separation of binding isotherms up to the relative fluorescence increase of ∼2.1. To obtain thermodynamically rigorous binding parameters, independent of any assumption about the relationship between the observed signal and the degree of binding, $\Sigma\Theta_i$, the fluorescence titration curves shown in Figure 2a have been

Table 1: Thermodynamic and Spectroscopic Parameters for the Binding of PriA Helicase to Different ssDNA Oligomers in Buffer C (pH 7.0, 10 °C) Containing 100 mM NaCl[a]

	10-mer dϵA(pϵA)$_9$	18-mer dϵA(pϵA)$_{17}$	26-mer dϵA(pϵA)$_{25}$	35-mer dϵA(pϵA)$_{34}$
K_N (M^{-1})	$(5.7 \pm 0.3) \times 10^4$	$(3.3 \pm 0.3) \times 10^4$	$(4.5 \pm 0.3) \times 10^4$	$(1.3 \pm 0.3) \times 10^5$
ΔF_1				1.25 ± 0.1
ΔF_{max}	2.85 ± 0.2	2.7 ± 0.2	2.5 ± 0.2	2.5 ± 0.2
ω				1.5 ± 0.5
$\partial \log K_N/\partial \log$[NaCl]	-2.4 ± 0.4	-3 ± 0.5	-3.3 ± 0.5	-4.1 ± 0.6
$\partial \log K_N/\partial \log$[NaBr]	-2.5 ± 0.4	-2.9 ± 0.5	-3.3 ± 0.5	-3.7 ± 0.6
$\partial \log \omega/\partial \log$[NaCl]				2.5 ± 0.8
$\partial \log \omega/\partial \log$[NaBr]				3.3 ± 0.8

[a] Errors are standard deviations determined using 3-4 independent titration experiments.

analyzed, using the approach outlined in Materials and Methods (*19*, *20*, *23*−*26*, *30*−*32*). Figure 2b shows the dependence of the observed relative fluorescence increase as a function of the average degree of binding, $\Sigma\Theta_i$, of the PriA helicase. The value of $\Sigma\Theta_i$ could be determined up to ~0.8. Short extrapolation to $\Delta F_{max} = 2.7 \pm 0.2$ gives the maximum value of $\Sigma\Theta_i = 0.9 \pm 0.1$. Analogous experiments at different salt concentrations examined in this work (see below) provide the same linear dependence of the observed signal as a function of the average degree of binding indicating that $\Sigma\Theta_i$ is independent of the salt concentration in the studied salt concentration range. The solid lines in Figure 2a are computer fits using eq 4, with a single set of binding parameters $K_{18} = (3.3 \pm 0.3) \times 10^4\ M^{-1}$ and $\Delta F_{max} = 2.7 \pm 0.2$ (Table 1).

There are two important aspects of the results shown in Figure 2, panels a and b. First, the 1:1 stoichiometry of dϵA(pϵA)$_{17}$ binding to the PriA protein is not affected by a ~19-fold increase of the ssDNA oligomer concentration (Figure 2a). The independence of the PriA−18-mer stoichiometry upon nucleic acid concentrations indicates that the enzyme has a single, strong binding site for ssDNA. If there is another weaker, functional binding site (sites), its affinity must be at least ~100 fold lower than the affinity of the strong binding site. The ~19-fold increase of the 18-mer concentration would detect such weak sites by showing an increase in the stoichiometry of the complex. Second, the 1:1 stoichiometry is preserved in low and high protein concentration ranges providing strong thermodynamic evidence that the helicase binds the ssDNA as a monomer. We determined, using the analytical ultracentrifugation technique, that the free protein exists in solution predominantly as a monomer in the large concentration range used in these studies (data not shown). On the other hand, as we mentioned above, titrations at high protein and nucleic acid concentrations are very difficult because of the propensity of the protein−nucleic acid complex to precipitate in these conditions (Figure 2a).

Salt Effect on PriA Helicase−dϵA(pϵA)$_{17}$ Interactions. The 18-mer, dϵA(pϵA)$_{17}$, encompasses the total site size of the PriA helicase−polymer ssDNA complex, thus, providing an opportunity to study the total site-size complex without any interference from the protein−protein interactions. Fluorescence titrations of dϵA(pϵA)$_{17}$ with the PriA helicase, in buffer C (pH 7.0, 10 °C) containing different NaCl concentrations, are shown in Figure 3a. Analogous titrations in the presence of NaBr are shown in Figure 3b. There is a decrease of the maximum fluorescence increase at saturation, ΔF_{max}, from 2.7 ± 0.2 at 100 mM to 1.5 ± 0.3 at 200 mM NaCl indicating changes in the structure of the nucleic acid in the complex as the salt concentration increases. The solid lines in Figure 3, panels a and b are computer fits to a single-site binding model, with two fitting parameters, intrinsic binding constant, K_{18}, and the maximum relative fluorescence increase, ΔF_{max} (eq 4). Figure 3c shows the dependence of the dϵA(pϵA)$_{17}$ intrinsic binding constant on NaCl and NaBr concentrations (log−log plots, 42−45). The plots are linear and characterized by the slopes $\partial \log K_{18}/\partial \log$[NaCl] $= -3 \pm 0.5$ and $\partial \log K_{18}/\partial \log$[NaBr] $= -2.9 \pm 0.5$, respectively. The values of both slopes indicate that there is a net release of ~3 ions upon the complex formation and the release is independent of the type of anion in solution. However, although the slopes are quite similar, there is an anion effect on the interactions reflected in the intrinsic binding constant, which is lower by a factor of ~1.3 in the presence of NaBr, when compared with the binding constant in the analogous NaCl concentrations (see Discussion).

PriA Helicase−dϵA(pϵA)$_9$ Interactions. The ssDNA-binding site of the PriA helicase is located within the central part of the enzyme molecule (Figure 1). The ssDNA-binding site encompasses only 8 ± 1 nucleotide residues, significantly less than the total site size of the protein−nucleic acid complex. To determine how interactions within the total ssDNA-binding site reflect the interactions with the ssDNA-binding site, we examined the binding of the 10-mer, dϵA(pϵA)$_9$, to the PriA helicase. Fluorescence titrations of dϵA(pϵA)$_9$ with the PriA helicase, in buffer C (pH 7.0, 10 °C) containing 100 mM NaCl, at different oligomer concentrations, are shown in Figure 4a. The dependence of the observed relative fluorescence increase as a function of the average degree of binding, $\Sigma\Theta_i$, of the PriA helicase on the 10-mer is shown in Figure 4b. The value of $\Sigma\Theta_i$ could be determined up to ~0.75. Short extrapolation to $\Delta F_{max} = 2.85 \pm 0.2$ gives the maximum value of $\Sigma\Theta_i = 1.1 \pm 0.15$. As observed in the case of the 18-mer, the 1:1 stoichiometry of the dϵA(pϵA)$_9$ binding to the PriA helicase is not affected by an ~37-fold increase of the nucleic acid oligomer concentration, indicating that there is one ssDNA-binding site on the enzyme. The solid lines in Figure 4a are computer fits using eq 4, with a single set of binding parameters, $K_{10} = (5.7 \pm 0.3) \times 10^4\ M^{-1}$ and $\Delta F_{max} = 2.85 \pm 0.2$ (Table 1). Notice that the value of the intrinsic binding constant, K_{10}, for the 10-mer is very similar to the K_{18}, indicating that the 10-mer forms all crucial contacts with the ssDNA-binding site of the enzyme. In other words, the area of the ssDNA-binding site engages significantly less nucleotide residues than the total site size of the complex in strong interactions (Figure 1).

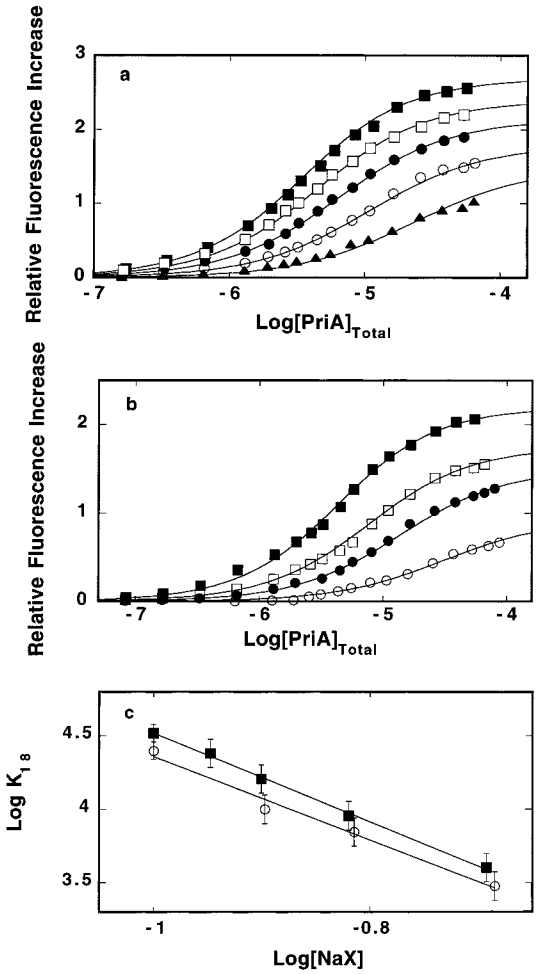

FIGURE 3: (a) Fluorescence titrations of the 18-mer, dϵA(pϵA)$_{17}$, with the PriA protein (λ_{ex} = 325 nm, λ_{em} = 410 nm) in buffer C (pH 7.0, 10 °C) containing different NaCl concentrations: 100 mM (■); 112.9 mM (□); 125.8 mM (●); 151.6 mM (○); and 203.1 mM (▲). The solid lines are computer fits of the titration curves, using a single-site binding isotherm (eq 4), that takes into account that the ssDNA-binding site of the enzyme engages only eight residues of the nucleic acid in direct interactions, with the intrinsic binding constant K_{18} and relative, maximum fluorescence increase ΔF_{max}: 3.3×10^4 M^{-1}, 2.7 (■); 2.4×10^4 M^{-1}, 2.4 (□); 1.6×10^4 M^{-1}, 2.15 (●); 9×10^3 M^{-1}, 1.8 (○); 4×10^3 M^{-1}, 1.5 (▲). (b) Fluorescence titrations of the 18-mer, dϵA(pϵA)$_{17}$, with the PriA protein (λ_{ex} = 325 nm, λ_{em} = 410 nm) in buffer C (pH 7.0, 10 °C) containing different NaBr concentrations: 100 mM (■); 126.7 mM (□); 153.7 mM (●); and 206.7 mM (○). The solid lines are computer fits of the titration curves, using a single-site binding isotherm (eq 4), with the intrinsic binding constant K_{18} and relative, maximum fluorescence increase ΔF_{max}: 2.5×10^4 M^{-1}, 2.2 (■); 1.3×10^4 M^{-1}, 1.75 (□); 7×10^3 M^{-1}, 1.5 (●); 3×10^3 M^{-1}, 0.93 (○). (c) Dependence of the logarithm of the intrinsic binding constants, K_{18}, upon the logarithm of NaCl (■) and NaBr (○) concentrations, determined from titrations shown in Figure 3, panels a and b. The solid lines are linear least-squares fits that provide the slopes $\partial \log K_{18}/\partial \log[\text{NaCl}] = -3 \pm 0.5$ and $\partial \log K_{18}/\partial \log[\text{NaBr}] = -2.9 \pm 0.5$, respectively.

To further address this issue, we studied the salt dependence of the 10-mer binding to the PriA helicase. Figure 5 shows the dependence of the dϵA(pϵA)$_9$ intrinsic binding constant on the logarithm of [NaCl] (log−log plot). The dependence of K_{10} upon [NaBr] is also included. The plots are linear and characterized by the slopes $\partial \log K_{10}/\partial \log[\text{NaCl}] = -2.4. \pm 0.4$ and $\partial \log K_{10}/\partial \log[\text{NaBr}] = -2.5 \pm 0.4$. The values of the slopes are slightly lower than those determined for the 18-mer (Figure 3c). Both slopes indicate that there

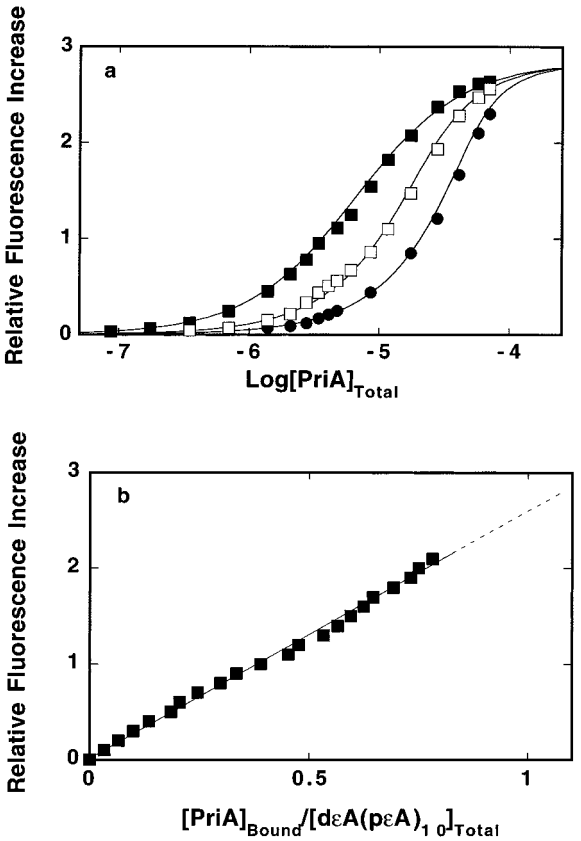

FIGURE 4: (a) Fluorescence titrations of the 10-mer dϵA(pϵA)$_9$ with the PriA protein (λ_{ex} = 325 nm, λ_{em} = 410 nm) in buffer C (pH 7.0, 10 °C), containing 100 mM NaCl, at three different nucleic acid concentrations: (■) 1.42×10^{-6}, (□) 8.12×10^{-6}, and (●) 1.92×10^{-5} M (oligomer). The solid lines are computer fits of the titration curves, using a single-site binding isotherm (eq 4), that takes into account the fact that the ssDNA-binding site engages only eight residues of the nucleic acid in direct interactions. Intrinsic binding constant $K_1 = 5.7 \times 10^4$ M^{-1} and relative fluorescence change $\Delta F_{max} = 2.85$. (b) Dependence of the relative fluorescence of the 10-mer, ΔF, upon the average number of bound PriA proteins (■). The solid line follows the experimental points and has no theoretical basis. The dashed line is the extrapolation of ΔF to the maximum value of $\Delta F_{max} = 2.85$.

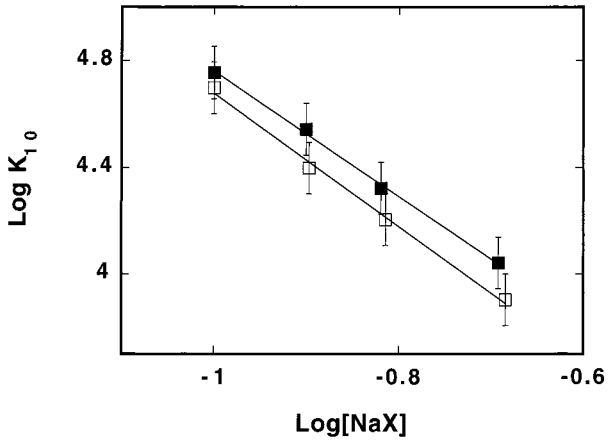

FIGURE 5: Dependence of the logarithm of the intrinsic binding constant, K_{10}, characterizing the PriA helicase−dϵA(pϵA)$_9$ complex upon the logarithm of NaCl (■) and NaBr (□) concentration in buffer C (pH 7.0, 10 °C). The solid lines are linear least-squares fits that provide the slopes $\partial \log K_{10}/\partial \log[\text{NaCl}] = -2.4 \pm 0.4$ and $\partial \log K_{10}/\partial \log[\text{NaBr}] = -2.5 \pm 0.4$, respectively.

is a net release of ∼2.5 ions upon the complex formation, and this number is independent of the type of anion in

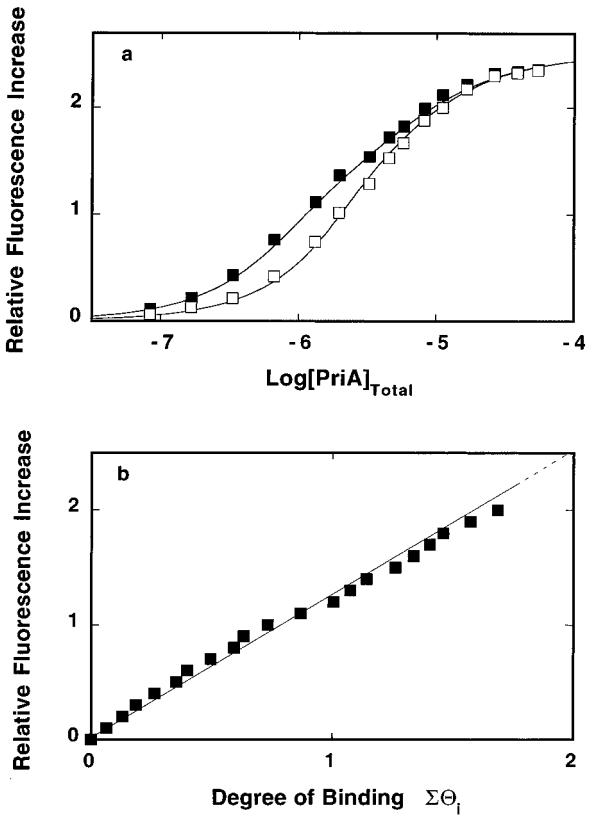

FIGURE 6: Fluorescence titrations of the 35-mer, dϵA(pϵA)$_{34}$,with the PriA protein (λ_{ex} = 325 nm, λ_{em} = 410 nm) in buffer C (pH 7.0, 10 °C), containing 100 mM NaCl at two different nucleic acid concentrations: (■) 4.7×10^{-7} and (□) 2.1×10^{-6} M. The solid lines are computer fits of the titration curves, using the statistical thermodynamic model for the binding of two PriA molecules to the 35-mer, described by eqs 7−11, using a single set of binding parameters: the intrinsic binding constant $K_{35} = 1.3 \times 10^5$ M^{-1}, cooperativity parameter $\omega = 1.5$, relative fluorescence change $\Delta F_1 = 1.25$, and $\Delta F_{max} = 2.5$. (b) Dependence of the relative fluorescence of the 35-mer, ΔF, upon the average number of bound PriA proteins (■). The solid line follows the experimental points and has no theoretical basis. The dashed line is the extrapolation of ΔF to the maximum value of $\Delta F_{max} = 2.5$.

solution. However, there is an anion effect on the interactions reflected in the intrinsic binding constant, slightly lower in the presence of NaBr, when compared with the binding constant in the presence of NaCl (Figure 5). The lower slopes, i.e., the lower number of the ions released upon the complex formation, as compared to the 18-mer, most probably reflect the lower thermodynamic degree of cation association with the ssDNA oligomers, as the size of the oligomer decreases (*42*, *44*). This conclusion is strongly supported by the fact that we observe a systematic increase in the number of ions released, as the number of nucleotide residues in the ssDNA oligomer increases (see below and Discussion).

Salt Effect on Intrinsic Affinity and Cooperativity of the PriA Helicase Binding to ssDNA. Experiments with 35-mer, dϵA(pϵA)$_{34}$. Fluorescence titrations of the 35-mer, dϵA-(pϵA)$_{34}$, with the PriA helicase, in buffer C (pH 7.0, 10 °C), containing 100 mM NaCl, at two different oligomer concentrations, are shown in Figure 6a. Careful inspection of the titration curves, particularly at a low nucleic acid concentration, reveals that the binding process is more complex with the isotherms extending over a larger protein concentration range than in the case of the 18- or 10-mer. The dependence of the observed relative fluorescence increase, as a function of the average degree of binding, $\Sigma\Theta_i$, of the PriA helicase on the 35-mer is shown in Figure 6b. The value of $\Sigma\Theta_i$ could be determined up to ~1.7. Short extrapolation to the maximum value of the fluorescence increase, $\Delta F_{max} = 2.5 \pm 0.2$, gives the maximum value of $\Sigma\Theta_i = 1.95 \pm 0.15$. Thus, two PriA molecules bind to the 35-mer. The plot is linear over the entire binding process, indicating that the binding of the first and second protein molecules induces the same nucleic acid fluorescence increase.

Quantitative analysis of the two PriA molecules binding to the 35-mer process must include intrinsic affinity, cooperative interactions between bound protein molecules, and the overlap between potential binding sites on the nucleic acid lattice (*38*−*41*). Moreover, we know that the number of nucleotide residues engaged in interactions with the ssDNA-binding site of the enzyme is only $m = 8$, and that the protein protrudes over a distance of 6 ± 1 nucleotides on both sides of the binding site (Figure 1). The isotherm for this binding system is described by eqs 7−11, with two fitting parameters, K_{35} and ω. The solid lines in Figure 6a are computer fits of the experimental isotherms using eqs 7−11 with a single set of binding parameters, $K_{35} = (1.3 \pm 0.3) \times 10^5$ M^{-1}, $\omega = 1.5 \pm 0.5$, and $\Delta F_{max} = 2.5 \pm 0.2$.

Fluorescence titrations of dϵA(pϵA)$_{34}$, with the PriA helicase in buffer C (pH 7.0, 10 °C), containing different NaCl concentrations, are shown in Figure 7a. It is evident that as the salt concentration increases both the macroscopic affinity and the maximum relative fluorescence change decrease. Essentially, the same behavior is observed when NaCl is replaced by NaBr (data not shown). The solid lines in Figure 7a are computer fits using eqs 7−11, and the obtained binding parameters are included in Table 2. The dependence of the intrinsic binding constant, K_{35}, upon the logarithm of [NaCl] and the logarithm of [NaBr] is shown in Figure 7b (log−log plot). Both plots are linear in the studied salt concentration range and are characterized by slopes $\partial \log K_{35}/\partial \log[NaCl] = -4.1 \pm 0.6$ and $\partial \log K_{35}/\partial \log[NaBr] = -3.7 \pm 0.6$, respectively. Thus, the intrinsic interactions between the PriA molecule and the nucleic acid lattice of the 35-mer are accompanied by the release of ~4 ions.

The effect of salt on the cooperative interactions is dramatically different. The dependence of the cooperativity parameter, ω, upon the logarithm of [NaCl] and the logarithm of [NaBr] is shown in Figure 7c. Because the values of ω are low, the error associated with their determination is significantly higher than in the case of the intrinsic binding constants. Nevertheless, the salt effect on the free energy of cooperative interactions between the two PriA molecules is characterized by the positive slope $\partial \log \omega/\partial \log[NaCl] = 2.5 \pm 0.8$ and $\partial \log \omega/\partial \log[NaBr] = 3.3 \pm 0.8$. Thus, cooperative interactions between the bound protein molecules are accompanied by an ion uptake not a release. Also, the larger value of $\partial \log \omega/\partial \log[NaBr]$ suggests that anions are a significant part of the ion uptake (see Discussion).

Magnesium Effect on the PriA Helicase−*ssDNA Interactions*. The stoichiometry of the PriA helicase−dϵA(pϵA)$_{17}$ complex has been examined in buffer C (pH 7.0, 10 °C) containing 100 mM NaCl and 1 mM $MgCl_2$ (data not shown). The average degree of binding, $\Sigma\Theta_i$, has been determined

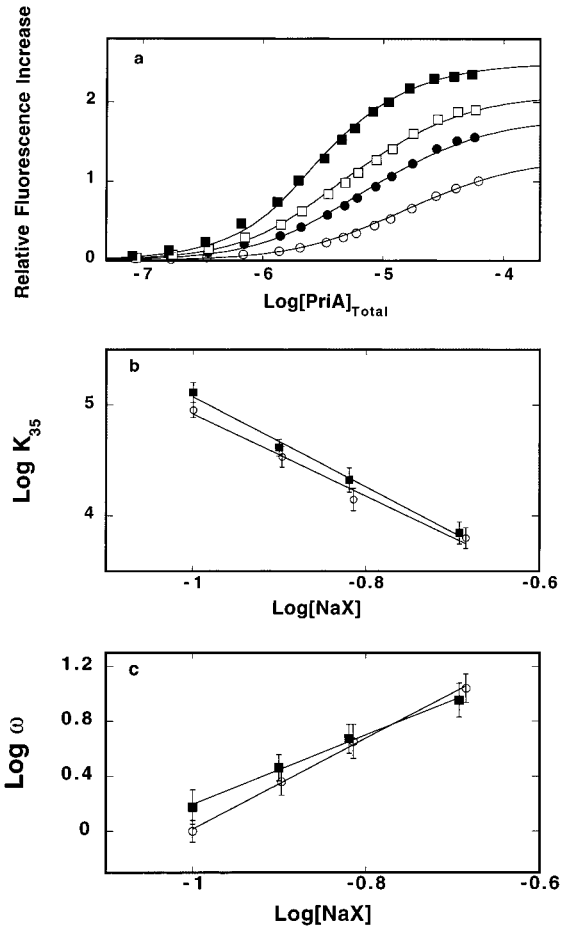

FIGURE 7: (a) Fluorescence titrations of the 35-mer, dϵA(pϵA)$_{34}$, with the PriA protein (λ_{ex} = 325 nm, λ_{em} = 410 nm) in buffer C (pH 7.0, 10 °C) containing different NaCl concentrations: 100 mM (■); 125.8 mM (□), 151.6 mM (●), 203.1 mM (○). The solid lines are computer fits of the titration curves, using the statistical thermodynamic model for the binding of two PriA molecules to the 35-mer, described by equations 7−11. The obtained binding parameters are included in Table 2. (b) Dependence of the logarithm of the intrinsic binding constants, K_{35}, upon the logarithm of NaCl (■) and NaBr (○) concentration. The solid lines are linear least-squares fits which provide the slopes $\partial\log K_{35}/\partial\log[\text{NaCl}] = -4.1 \pm 0.6$ and $\partial\log K_{35}/\partial\log[\text{NaBr}] = -3.7 \pm 0.6$, respectively. (c) Dependence of the logarithm of the cooperativity parameter ω upon the logarithm of NaCl (■) and NaBr (○) concentration. The solid lines are linear least-squares fits which provide the slopes $\partial\log \omega/\partial\log[\text{NaCl}] = 2.5 \pm 0.8$ and $\partial\log \omega/\partial\log[\text{NaBr}] = 3.3 \pm 0.8$, respectively.

using the quantitative approach described in Materials and Methods. Extrapolation of the plot of the observed ΔF as a function of $\Sigma\Theta_i$ to $\Delta F_{max} = 2.8 \pm 0.2$ gives the maximum value of $\Sigma\Theta_i = 0.9 \pm 0.15$. Thus, the presence of Mg^{2+} ions does not affect the stoichiometry of the PriA protein−nucleic acid complex. Analytical ultracentrifugation studies showed that the protein preserves its monomeric state in solution in the presence of magnesium (data not shown).

A series of fluorescence titrations of dϵA(pϵA)$_{17}$ with the PriA helicase, in buffer C (pH 7.0, 10 °C), containing 100 mM NaCl and different $MgCl_2$ concentrations, are shown in Figure 8a. Both macroscopic affinity and ΔF_{max} decrease as a result of the magnesium concentration increase. The solid lines in Figure 8a are computer fits to a single-site binding model, with two fitting parameters, intrinsic binding constant, K_{18}, and ΔF_{max} (eq 4). Figure 8b shows the

Table 2: Thermodynamic and Spectroscopic Parameters of the PriA Helicase Binding to the 35-mer dϵA(pϵA)$_{34}$ in Buffer C (pH 7.0, 10 °C) at Different NaCl and NaBr Concentrations[a]

	K_{35}	ω	ΔF_1	ΔF_{max}
		NaCl (M)		
0.1	$(1.3 \pm 0.3) \times 10^5$	1.5 ± 0.5	1.25 ± 0.1	2.5 ± 0.2
0.126	$(4.1 \pm 08) \times 10^4$	2.9 ± 0.8	1.1 ± 0.1	2.1 ± 0.2
0.152	$(2.1 \pm 0.6) \times 10^4$	4.7 ± 1.3	0.9 ± 0.1	1.8 ± 0.2
0.203	$(7 \pm 1.7) \times 10^3$	9 ± 3	0.7 ± 0.1	1.3 ± 0.2
		NaBr (M)		
0.1	$(9 \pm 1.5) \times 10^4$	1 ± 0.2	1.4 ± 0.1	2.8 ± 0.2
0.127	$(3.4 \pm 0.8) \times 10^4$	2.3 ± 0.6	1.2 ± 0.1	2.4 ± 0.2
0.153	$(1.4 \pm 0.4) \times 10^4$	4.5 ± 1.5	0.9 ± 0.1	1.8 ± 0.3
0.207	$(6.3 \pm 1.5) \times 10^4$	11 ± 3	0.5 ± 0.1	1.1 ± 0.2

[a] See text for details. Errors are standard deviations determined using 3−4 independent titration experiments.

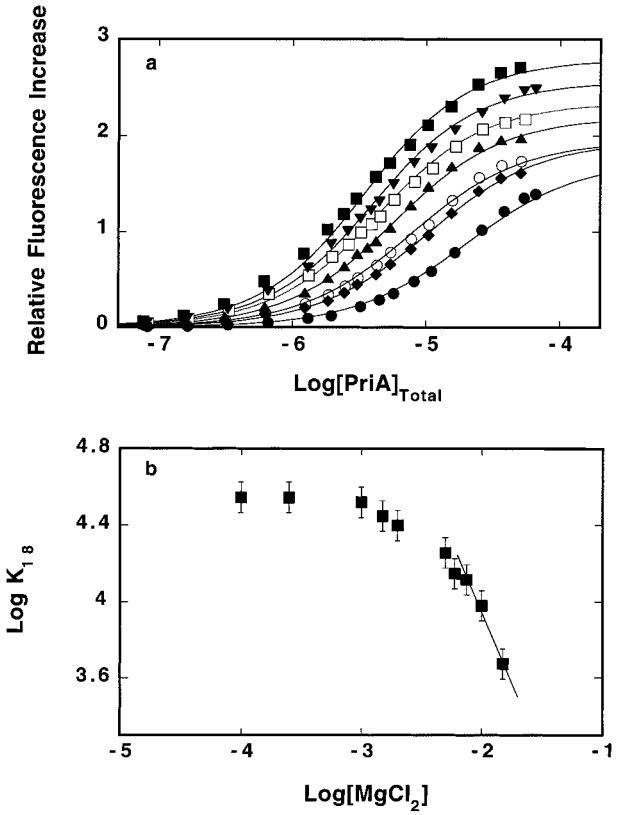

FIGURE 8: (a) Fluorescence titrations of the 18-mer, dϵA(pϵA)$_{17}$, with the PriA protein (λ_{ex} = 325 nm, λ_{em} = 410 nm) in buffer C (pH 7.0, 10 °C), containing 100 mM NaCl and different $MgCl_2$ concentrations: 1 mM (■); 1.5 mM (▼); 2 mM (□); 5 mM (▲); 7.5 mM (○); 10 mM (◆); and 15 mM (●). The solid lines are computer fits of the titration curves, using a single-site binding isotherm (eq 4), that take into account that the ssDNA-binding site of the enzyme engages only eight residues of the nucleic acid in direct interactions with the intrinsic binding constant, K_{18}, and the relative, maximum fluorescence increase, ΔF_{max}: 5.7×10^4 M^{-1}, 2.85 (■); 3.3×10^4 M^{-1}, 2.8 (▼); 2.5×10^4 M^{-1}, 2.35 (□); 1.8×10^4 M^{-1}, 2.2 (▲); 1.3×10^4 M^{-1}, 1.95 (○); 9.5×10^3 M^{-1}, 1.95 (◆); 4.7×10^3 M^{-1}, 1.75 (●). (b) Dependence of the logarithm of the intrinsic binding constant, K_{18}, upon the logarithm of $MgCl_2$ concentration (■). The solid line, through the linear part of the plot in the high $MgCl_2$ concentration range, is the linear least-squares fit which provides the slopes $\partial\log K_{18}/\partial\log[MgCl_2] = -1.5 \pm 0.3$.

dependence of the dϵA(pϵA)$_{17}$ intrinsic binding constant on the logarithm of [$MgCl_2$] (log−log plot). The plot is clearly nonlinear. At low magnesium concentrations, the slope, $\partial\log K_{18}/\partial\log[MgCl_2] = \sim 0 \pm 0.2$. Above ~1 mM $MgCl_2$, the

affinity dramatically decreases, indicating that the intrinsic binding process is accompanied by a net release of ions. At high magnesium concentrations, the linear part of the plot is characterized by the $\partial \log K_{18}/\partial \log[MgCl_2] = -1.5 \pm 0.3$, which is significantly lower than -3 ± 0.5 obtained in the presence of NaCl alone (Figure 3c, see Discussion).

Base Specificity of PriA−ssDNA Interactions. Lattice Competition Titrations Using the MCT Method. Determination of the affinities of the PriA helicase for unmodified ssDNAs, using the MCT method, is based on the same thermodynamic arguments as applied to titrations of fluorescent nucleic acids with the protein (eqs 5 and 6) (*20*, *34*). In the presence of the competing ssDNA oligomer, the enzyme binds to two different nucleic acids that are present in the solution, but the observed signal originates only from the fluorescent "reference" lattice. In studies described in this work we use, as a reference lattice, the 18-mer, dϵA-(pϵA)$_{17}$, and the base specificity of the PriA helicase has been examined using different nonfluorescent, competing 20-mers, dN(pN)$_{19}$. Both lattices bind a single protein molecule with only eight nucleotide residues engaged in the direct interactions with the protein.

The binding system considered here is composed of two short nucleic acid lattices, dϵA(pϵA)$_{17}$ and dN(pN)$_{19}$, which can accommodate only a single molecule of the protein. The partition function, Z, of the entire binding system is defined as

$$Z = 1 + (N_R - m + 1)K_{18}P_F + (N_S - m + 1)K_{20}P_F \quad (12)$$

where $N_R = 18$ and $N_S = 20$, K_{20} is the intrinsic binding constant of the ligand for the 20-mer. The concentration of the bound ligand, P_b, is defined as

$$P_b = \left[\frac{(N_R - m + 1)K_{18}P_F}{1 + (N_R - m + 1)K_{18}P_F}\right]M_{T_R} + \left[\frac{(N_S - m + 1)K_{20}P_F}{1 + (N_S - m + 1)K_{20}P_F}\right]M_{T_S} \quad (13)$$

$$P_b = (\sum \Theta_i)_R M_{T_R} + (\sum \Theta_i)_S M_{T_S} \quad (14)$$

$$P_F = P_T - P_b \quad (15)$$

where P_T is the total concentration of the ligand and M_{T_R} and M_{T_S} are the total concentrations of the 18- and 20-mers, respectively.

Fluorescence titrations of dϵA(pϵA)$_{17}$ with the PriA protein, in buffer C (pH 7.0, 10 °C) containing 100 mM NaCl, in the presence of two different dT(pT)$_{19}$ concentrations, are shown in Figure 9a. For comparison, the titration curve in the absence of the competing 20-mer is also included. A significant shift of the binding isotherm, with increasing dT(pT)$_{19}$ concentrations, indicates strong competition between dϵA(pϵA)$_{17}$ and dT(pT)$_{19}$ for the PriA helicase. The dependence of the observed fluorescence increase upon the average number of PriA molecules bound per dT(pT)$_{19}$ molecule, $(\Sigma\Theta_i)_S$, is shown in Figure 9b. At $\Delta F \sim 1.4$, the plot reaches the stoichiometry of 1 ± 0.1 PriA monomer bound/dT(pT)$_{19}$ molecule, a clear indication that the enzyme has higher affinity for dT(pT)$_{19}$ than for the reference dϵA-(pϵA)$_{17}$ (*20*). A further increase of the PriA concentration

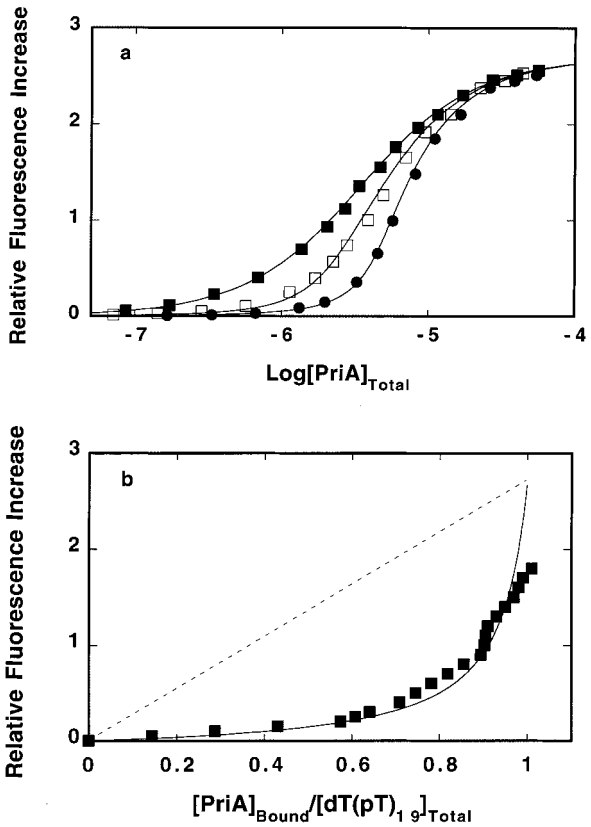

FIGURE 9: (a) Fluorescence titrations of the 18-mer, dϵA(pϵA)$_{17}$, with the PriA protein ($\lambda_{ex} = 325$ nm, $\lambda_{em} = 410$ nm) in buffer C (pH 7.0, 10 °C) containing 100 mM NaCl and two different concentrations (oligomer) of the 20-mer, dT(pT)$_{19}$: 1.5×10^{-6} (□) and 3.86×10^{-6} M (●). Titration of the 18-mer alone at the same oligomer concentration (1.42×10^{-6} M) and in the same buffer conditions is also included (■). The solid lines are computer fits of the binding isotherms using eqs 12−15 (lattice competition titrations) with the intrinsic binding constant for $K_{20} = 4.5 \times 10^4$ M^{-1}. (b) Dependence of the observed relative fluorescence increase of dϵA(pϵA)$_{17}$ upon the average number of the PriA molecules bound per 20-mer, dT(pT)$_{19}$. The average number of the PriA molecules bound per 20-mer has been determined using the MCT method (Materials and Methods). The solid line is the computer simulation of the dependence of the observed relative fluorescence increase upon the average number of the bound PriA molecules per dT(pT)$_{19}$ using the independently determined intrinsic binding constants for both the PriA−dϵA(pϵA)$_{17}$ and PriA−dT(pT)$_{19}$ complexes in the same solution conditions.

does not change the determined stoichiometry of the PriA−dT(pT)$_{19}$ complex. The observed increase of the dϵA(pϵA)$_{17}$ fluorescence results from continuing the binding of the PriA protein to the 18-mer, after the saturation of dT(pT)$_{19}$ has been reached (*20*).

The solid lines in Figure 9a are computer fits of the experimental isotherms, with a single fitting parameter, K_{20}, using eqs 12−15. For dT(pT)$_{19}$, the obtained value of $K_{20} = (4.5 \pm 0.4) \times 10^5$ M^{-1}. The solid line in Figure 9b is the computer simulation of the dependence of the observed fluorescence increase upon the average number of PriA monomers bound per dT(pT)$_{19}$, using the independently determined binding constants for both the PriA−dϵA(pϵA)$_{17}$ and PriA−dT(pT)$_{19}$ complexes in the same solution conditions. Analogous studies have been performed for other unmodified 20-mers and the determined intrinsic binding constants are included in Table 3. The results indicate that the PriA helicase shows a preference toward pyrimidine

Table 3: Macroscopic and Intrinsic Binding Constants K_{20}^{M} and K_{20} Characterizing Complex Formation between the PriA Helicase and Different ssDNA Homo-oligomers, dN(pN)$_{19}$, in Buffer C (pH 7.0, 10 °C), Containing 100 mM NaCl[a]

	dϵA(pϵA)$_{19}$	dA(pA)$_{19}$	dT(pT)$_{19}$	dC(pC)$_{19}$
K_{20} (M^{-1})	$(4 \pm 0.4) \times 10^4$	$(3 \pm 0.4) \times 10^4$	$(4.5 \pm 0.4) \times 10^5$	$(4 \pm 0.5) \times 10^5$
K_{20}^{M} (M^{-1})	$(5.2 \pm 0.5) \times 10^5$	$(3.9 \pm 0.5) \times 10^5$	$(5.9 \pm 0.7) \times 10^6$	$(5.2 \pm 0.7) \times 10^6$

[a] The values of K_{20} for the unmodified 20-mers have been determined using the MCT Method (see text for details). Errors are standard deviations determined using 3−4 independent titration experiments.

oligomers with the intrinsic binding constants for dT(pT)$_{19}$ and dC(pC)$_{19}$ being ~1 order of magnitude larger than the corresponding intrinsic binding constants for dA(pA)$_{19}$ and dϵA(pϵA)$_{19}$, respectively (Table 3).

Nucleotide Cofactor Effect on the PriA Helicase Interactions with ssDNA. The thermodynamic studies described above concentrated on the quantitative characterization of the PriA helicase interactions with the ssDNA in the absence of the nucleotide cofactors. The ATPase activity of the enzyme is only efficiently stimulated by a specific, primosome assembly site sequence, PAS, with the nonspecific ssDNA being significantly less efficient (*7, 8, 11, 12*). To address the issue of the nucleotide effect on the enzyme interactions with the ssDNA exclusively in the ground state, without catalysis, we used the ATP nonhydrolyzable analogue, AMP-PNP.

Fluorescence titrations of the 18-mer, dϵA(pϵA)$_{17}$, with the PriA helicase, in buffer C (pH 7.0, 10 °C), containing 100 mM NaCl, 5 mM $MgCl_2$, and 5×10^{-4} M AMP-PNP at different oligomer concentrations, are shown in Figure 10a. The AMP-PNP concentration selected for these studies ensures that the nucleotide binding of the helicase is fully saturated with the nucleotide cofactor (M. Jezewska, unpublished data). The dependence of the observed relative fluorescence increase as a function of the average degree of binding, $\Sigma\Theta_i$, of the PriA helicase is shown in Figure 10b. The value of $\Sigma\Theta_i$ could be determined up to ~0.75. Extrapolation of the plot to $\Delta F_{max} = 3.6 \pm 0.3$ gives the maximum value of $\Sigma\Theta_i = 0.95 \pm 0.1$. Thus, the presence of the ATP analogue does not affect the stoichiometry of the protein−nucleic acid complex; however, it does affect the affinity of the enzyme for the ssDNA and the structure of the nucleic acid in the complex. The solid lines in Figure 10a are computer fits of the experimental isotherms to eq 4, with a single set of two parameters, K_{18} and ΔF_{max}. The obtained value of $K_{18} = (8 \pm 0.3) \times 10^3$ M^{-1}, which is a factor of ~4 lower than the value obtained in the absence of AMP-PNP (Table 1, Figure 3a). The value of $\Delta F_{max} = 3.6 \pm 0.3$ is significantly higher than $\Delta F_{max} = 2.2 \pm 0.2$ obtained in the same solution conditions, but in the absence of the ATP analogue (Figure 2a). The results show that despite the lower affinity, the ATP analogue affects the structure of the nucleic acid in the binding site. Fluorescence titrations of the 18-mer, dϵA(pϵA)$_{17}$, with the PriA helicase, in buffer C (pH 7.0, 10 °C), containing 100 mM NaCl, 5 mM $MgCl_2$, in the presence of 5×10^{-4} M AMP-PNP, 5×10^{-4} M ADP, and in absence of nucleotide cofactors are shown in Figure 11. While AMP-PNP significantly affects interactions of the helicase with the ssDNA, the ADP has no detectable effect in the studied solution conditions, although it binds the helicase with an affinity similar to that of the ATP analogue (M. Jezewska, unpublished data).

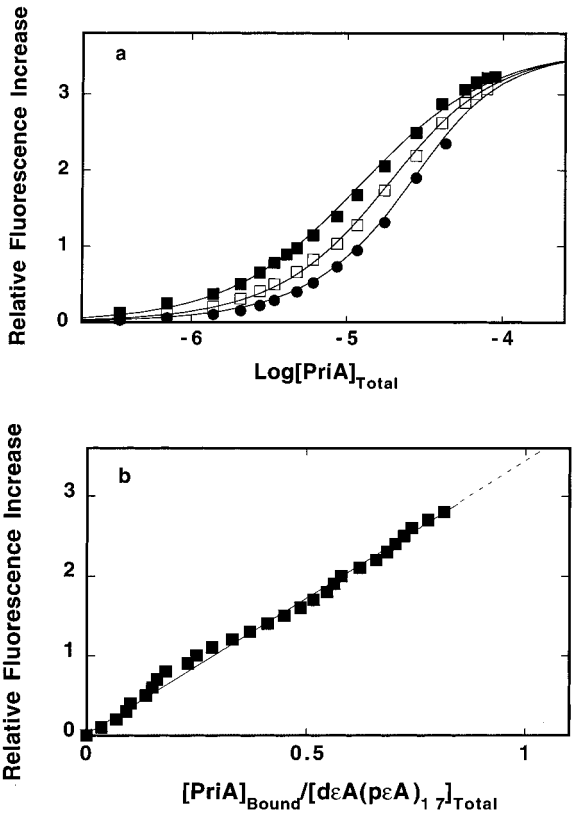

FIGURE 10: (a) Fluorescence titrations of the 18-mer, dϵA(pϵA)$_{17}$, with the PriA protein (λ_{ex} = 325 nm, λ_{em} = 410 nm) in buffer C (pH 7.0, 10 °C), containing 100 mM NaCl, 5 mM $MgCl_2$, and 5×10^{-4} M AMP-PNP, at three different nucleic acid concentrations: (■) 1.42×10^{-6}, (□) 1.35×10^{-5}, and (●) 2.71×10^{-5} M (oligomer). The solid lines are computer fits of the titration curves, using eq 4 with the intrinsic binding constant $K_{18} = 8 \times 10^3$ M^{-1} and relative fluorescence change $\Delta F_{max} = 3.6$. (b) Dependence of the relative fluorescence of the 18-mer, ΔF, upon the average number of bound PriA proteins (■). The solid line follows the experimental points and has no theoretical basis. The dashed line is the extrapolation of ΔF to the maximum value of $\Delta F_{max} = 3.6$.

DISCUSSION

The Stoichiometry of the PriA Helicase−ssDNA Complex Is Independent of the Type of Nucleic Acid Base, Salt Concentration, Type of Salt, and Nucleotide Cofactors. The physiological role of the PriA helicase is strictly related to the ability of the enzyme to interact with both ss and dsDNAs (*1−3*). Yet, little or nothing is known about the quantitative molecular mechanism of the PriA helicase−nucleic acid interactions. In this communication, we provide quantitative studies of PriA helicase interactions with the ssDNA.

Both direct binding studies of the PriA helicase to etheno derivatives of the ssDNA and competition experiments with unmodified, nonfluorescent ssDNAs, in different solution conditions, indicate that the PriA protein binds the nucleic acid as a monomer. This is particularly evident in fluorescence titrations performed at very different concentrations of the fluorescent ssDNA oligomers, as shown in Figures 2 and 4. Independently of the protein concentration range used in the stoichiometry determinations (Figures 2 and 4), the stoichiometry of 1:1 of PriA−oligomer complexes with dϵA-

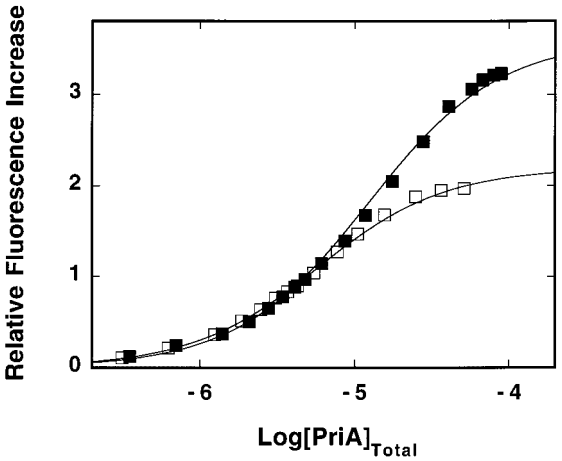

FIGURE 11: Fluorescence titrations of the 18-mer, dϵA(pϵA)$_{17}$, with the PriA protein (λ_{ex} = 325 nm, λ_{em} = 410 nm) in buffer C (pH 7.0, 10 °C), containing 100 mM NaCl, 5 mM $MgCl_2$, and 5 × 10^{-4} M AMP-PNP (■) or 5 × 10^{-4} M ADP (□). The concentration of dϵA(pϵA)$_{17}$ is 1.42 × 10^{-6} M (oligomer). The solid lines are computer fits of the titration curves, using eq 4 with the intrinsic binding constant K_{18} = 1.8 × 10^4 M^{-1} and ΔF_{max} = 2.2 in the absence and presence of ADP, and K_{18} = 8 × 10^3 M^{-1} and ΔF_{max} = 3.6 in the presence of AMP-PNP.

(pϵA)$_{17}$ and dϵA(pϵA)$_9$ remains the same. Moreover, the constant 1:1 stoichiometry of the formed complexes is also evident in the adequate fits of the experimental titration curves to the theoretical isotherms describing the binding of a single protein molecule to the oligomers. The same is true for the competition studies with unmodified ssDNA oligomers and the titrations in the presence of $MgCl_2$ and nucleotide cofactors. Thus, the PriA helicase binds the ssDNA as a monomer, independently of the type of nucleic acid base, as well as salt concentrations, type of salt, and cofactors. However, it should be pointed out that in equilibrium studies it is the stoichiometry of the ground state of the enzyme−ssDNA complex that is measured without the catalysis, i.e., without ATP hydrolysis or duplex DNA unwinding by the helicase. It may still be possible that catalytic activity of the PriA helicase requires an additional enzyme molecule as is the case for the *E. coli* rep helicase (*17*).

PriA Helicase Has a Single ssDNA Binding Site. As we mentioned above, binding of the PriA protein to the 18-mer dϵA(pϵA)$_{17}$ shows that even an ∼19-fold increase of the oligomer concentration does not change the 1:1 stoichiometry of the complex (Figure 2a). A similar effect is observed in the case of the enzyme binding to the 10-mer, dϵA(pϵA)$_9$. These results indicate that the enzyme has a single ssDNA-binding site. If there are other binding sites, their affinity must be ∼2 orders of magnitude lower than the affinity of the strong site. Moreover, titrations in the presence of the unmodified ssDNA oligomers show strong competition for the single binding site and not mutual binding to the protein. We also examined the competition between the polymer ssDNA and ssDNA oligomers (data not shown). Although we could not reach the saturation of the polymer DNA because of the precipitation of the complex in the high protein and DNA concentrations, they showed that the oligomers compete very efficiently with poly(dϵA) for the enzyme. Thus, the same binding site is used when PriA binds to polymer or oligomer ssDNAs.

The Intrinsic Affinity of the PriA Protein−ssDNA Interactions Depends on the Type of Nucleic Acid Base. Binding of the PriA helicase to the unmodified ssDNA is not accompanied by adequate protein fluorescence changes to perform quantitative analyses of the energetics of the complex formation. However, application of the MCT method allowed us to quantitatively address the intrinsic affinity of the PriA helicase for unmodified ssDNAs (*20*, *34*). There is a significant difference in the intrinsic affinity of the PriA helicase for the ssDNA, differing by the type of base. The enzyme shows ∼1 order of magnitude higher intrinsic affinity for pyrimidine oligomers than for purine oligomers, which indicates an important contribution of the base in ssDNA binding (Table 3). Higher intrinsic affinities of the PriA helicase for pyrimidine oligomers is different from the other *E. coli* replicative helicase, the DnaB protein (*34*). Thus, the intrinsic binding constant of the DnaB protein for poly(dA) is 2 orders of magnitude higher than the binding constant for poly(dT) (*34*). Such opposite behavior suggests a difference in the structures of the ssDNA-binding sites, which may reflect the differences in the physiological activities and possibly different mechanisms of functioning of PriA and DnaB. The PriA helicase recognizes a specific sequence of the primosome assembly site (PAS), which stimulates ATPase activity and from which the enzyme initiates the dsDNA unwinding in the 3′ → 5′ direction (*3*). The ATPase activity of DnaB is stimulated by a nonspecific ssDNA. The enzyme can initiate unwinding in the sequence independent manner and unwinds the dsDNA in the 5′ → 3′ direction (*1*, *2*, *17*, *18*).

Salt Effect on the Intrinsic Affinity of the PriA Helicase−ssDNA Complex Results Predominantly From Interactions Between the ssDNA-Binding Site of the Enzyme and the Nucleic Acid. Our current model of the PriA helicase−ssDNA complex is depicted in Figure 1. The total site size of the complex is $n = 20 \pm 3$ nucleotide residues. However, the ssDNA-binding site of the enzyme engages only $m = 8 \pm 1$ residues in direct interactions. In this model, all crucial contacts between the protein and the DNA, which contribute to the intrinsic affinity, are contained in the ssDNA-binding site. The protein engages only 8 ± 1 residues in direct interactions, independently of the length of the ssDNA oligomer, and has a similar intrinsic affinity for ssDNA oligomers of different lengths, as long as the oligomer is long enough to encompass the ssDNA-binding site. The protruding protein matrix over the remaining residues of the total site size of the complex does not form interacting contacts with the nucleic acid and does not contribute to the intrinsic affinity as experimentally observed (Table 1).

Salt dependence of the intrinsic affinities of the PriA helicase for the 18-mer, which encompasses the total site size of the complex and with the 10-mer, which is long enough to bind only to the ssDNA-binding site of the enzyme, provides strong support for this model. The slope $\partial \log K_{18}/\partial \log[NaCl] = -3 \pm 0.5$ for the 18-mer, dϵA(pϵA)$_{17}$, and $\partial \log K_{10}/\partial \log[NaCl] = -2.4 \pm 0.4$ for the 10-mer dϵA(pϵA)$_9$. Although there is a slight increase of the absolute value of the slope between the 18- and 10-mer (see below), such a small difference cannot account for the 80% difference in the length between both oligomers. The 18-mer can access a much larger area of the protein and form ion-dependent

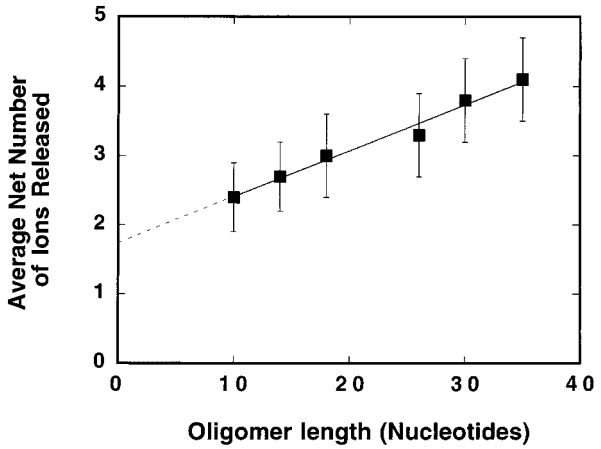

FIGURE 12: Dependence of the net absolute number of released ions accompanying the intrinsic interaction between the PriA helicase and the ssDNA oligomers, $|\partial \log K_N/\partial \log[NaCl]|$, upon the number of nucleotide residues in the nucleic acid. The solid line is the linear least-squares fit of the plot. The dashed line is a linear extrapolation to $N = 0$ that gives the value 1.75 ± 0.5 (see text for details).

interactions outside the ssDNA-binding site. The similar values of the log−log plot slopes indicate that a similar number of ions is released in both complexes, independently as to whether the protein interacts with the ssDNA oligomer encompassing the total site size or with the oligomer exclusively binding to the ssDNA-binding site.

Bromide anions, Br^-, are known to have significantly higher affinity for protein amine groups than Cl^- (*45*). The slopes $\partial \log K_{18}/\partial \log[NaBr] = -2.9 \pm 0.4$ for the 18-mer, dϵA(pϵA)$_{17}$, and $\partial \log K_{10}/\partial \log[NaBr] = -2.5 \pm 0.4$ for the 10-mer dϵA(pϵA)$_9$, also indicating that the anion effect on the studied interactions is very similar for both oligomers. Thus, the very similar number of ions released, when NaCl is replaced by NaBr, indicates that any anion release accompanying the complex formation depends little on the length of the ssDNA oligomer. In other words, the salt in solution affects the thermodynamics of the enzyme interactions with the ssDNA independently of the length of the ssDNA oligomer. The simplest explanation of this effect is that in all complexes the same number of nucleotide residues are engaged in direct interactions with the protein, as proposed by the model in Figure 1.

However, we observed an interesting, increasing trend in the value of slopes, $\partial \log K_N/\partial \log[NaCl]$ and $\partial \log K_N/\partial \log[NaBr]$, as the length of the ssDNA oligomer increases (Table 1). The dependence of the absolute values of the slope, $\partial \log K_N/\partial \log[NaCl]$, upon the number of nucleotide residues of the oligomer is shown in Figure 12. In this plot, we also added results for other ssDNA oligomers, not extensively discussed in this work. There is a clear empirical, linear dependence between the net number of ions released in the intrinsic interactions and the length of the oligomer. Extrapolation of the plot to $N = 0$ gives the length-independent value of 1.7 ± 0.5. With the assumption that increasing salt concentrations affect only cation and anion exchanges, the slope of the log−log plot for the protein−nucleic acid interactions can be defined by the linkage relationship, $\partial \log K_N/\partial \log[NaCl] = -p - q$, where p and q are the average net numbers of cations and anions released upon the complex formation (*42*, *43*).

The empirical linear dependence of the number of ions released in the intrinsic interaction between the PriA helicase and ssDNA oligomers can be semiqualitatively understood by taking into account that the thermodynamic degree of cation binding per phosphate group of the ssDNA, ψ, depends on the length of the nucleic acid (*42*, *43*). Using the quantity, ψ, the slope of the log−log plot is defined by the linkage relationship, $\partial \log K_N/\partial \log[NaCl] = -n\psi - q$, where n is the number of ionic interactions between the protein and the nucleic acid (*42*, *43*). Because of the oligomeric nature of the ssDNA oligomers, the value of ψ of the ssDNA oligomers is lower than that of the polymer DNA and decreases as the length of the oligomer decreases (*43*, *45*). Recall that each oligomer included in Figure 12 forms all crucial contacts with the PriA ssDNA-binding site, as expressed by similar intrinsic binding constants (see above). The only factor in the equation that should be affected by the changing length of the nucleic acid is ψ. The linear dependence would result from the fact that ψ decreases toward zero, for short oligomers in an approximately linear fashion, as the length of the oligomer decreases (*44*). In the simplest situation, the length-independent factor $q = 1.7 \pm 0.5$ would then be equal to the number of anions released in the complex formation, although it may contain additional factors, e.g., net proton release (*42*, *43*). Thus, this analysis suggests that the release of 1−2 anions may accompany the intrinsic interactions. In this context, the apparent independence of the slope of all studied complexes between PriA and ssDNA oligomers upon the type of anion in solution could result from the fact that in the studied salt concentration range (>100 mM) all anion binding sites are fully saturated with chloride or bromide ions.

Contrary to monovalent salts, the log−log plot in the presence of $MgCl_2$ is clearly nonlinear (Figure 8b). Because the thermodynamic degree of Mg^{2+} binding on the 18-mer changes in the studied salt concentration ranges, the nonlinear behavior of the log−log plot suggests that the released ions may predominantly originate from the nucleic acid (*43*). Thus, the lower absolute value of the slope of the linear part of the plot, as compared to NaCl or NaBr, is expected because of the lower value of ψ for magnesium cations (*42*, *43*). It should be mentioned that because of the presence of multiple components in solution, the studied system is extremely complex. Nevertheless, a strong decrease of the intrinsic binding constant of the PriA protein−18-mer complex occurs around 1 mM $MgCl_2$ and suggests that the ions are released from binding sites that are characterized by the affinity constant of at least 500 M^{-1}.

Cooperative Interactions Between Bound PriA Molecules Are Accompanied by an Ion Uptake. Binding of the PriA helicase to the ssDNA is characterized by a low value of the cooperativity parameter, ω, which increases with the increase of the salt concentrations (Table 2). Thus, contrary to the intrinsic affinities, the cooperative interactions are accompanied by a net ion binding. The slope $\partial \log \omega/\partial \log[NaCl] = 2.5 \pm 0.8$ indicates that there is a net uptake of 2−3 ions accompanying the cooperative interactions. The value of $\partial \log \omega/\partial \log[NaBr] = 3.3 \pm 0.8$ is higher than $\partial \log \omega/\partial \log[NaCl]$, indicating that anions participate in the net ion uptake. The fact that the uptake includes anions strongly suggests that the parameter ω characterizes weak protein−

protein interactions between bound PriA monomers. Weak cooperative interactions clearly show that the PriA helicase, like the *E. coli* DnaB helicase, is not able to form long protein clusters when bound to the ssDNA. As we pointed out before, this property may reflect a general aspect of the functioning of a replicative helicase that does not require long protein clusters to perform its functions (*19*, *20*, *34*). On the other hand, the fact that ω increases with the increase of salt concentration suggests that cooperative interactions may play a role in PriA helicase activities, particularly in the vicinity of the DNA where a strong accumulation of cations occurs (*42*−*44*).

Nucleotide Cofactors Do Not Significantly Affect the Affinity of the PriA Helicase Toward the ssDNA. A common feature of the well-studied helicases, the *E. coli* DnaB protein, Rep helicase, phage T7, and T4 helicases is that their affinities toward the ssDNA are dramatically affected by the presence of nucleotide cofactors in solution (*47*−*51*). In the case of the DnaB helicase, the affinity of the enzyme for the ssDNA increases $\sim 10^5$ fold in the presence of AMP-PNP, as compared to the conditions without cofactors in which the affinity of the enzyme for the ssDNA is barely detectable (*49*). In this context, the PriA helicase is strikingly different. The enzyme binds the ssDNA with significant affinity in the absence of any nucleotide cofactors (see above). Moreover, the presence of AMP-PNP diminishes the intrinsic affinity of the PriA protein for the ssDNA by a factor of $\sim$4, while ADP has no detectable effect (Figure 12).

The control of the ssDNA and dsDNA affinities of a helicase by ATP binding, or binding and hydrolysis, has been a key element in the proposed mechanisms of the enzyme functioning (*1*, *17*, *18*). Particularly, the binding and release of the DNA substrates, as a function of the dynamics of the reaction at the nucleotide binding sites, are viewed as paramount for the free energy transduction and mechanical translocation of the enzymes along the nucleic acid lattice (*17*). The results obtained in this work provide an indication that the mechanism by which the PriA helicase operates may be different from other helicases that have been examined so far. Most probably, such different behavior is related to the fact that the PriA helicase, contrary to other well-studied enzymes, requires a specific PAS sequence to efficiently initiate ATP hydrolysis and duplex DNA unwinding.

ACKNOWLEDGMENT

We thank Mrs. Gloria Drennan Davis for her help in preparing the manuscript.

REFERENCES

1. Kornberg, A., and Baker, T. A. (1992) *DNA Replication*, W. H. Freeman, San Francisco.
2. Marians, K. J. (1992) *Annu. Rev. Biochem. 61*, 673−719.
3. Marians, K. J. (1999) *Prog. Nucl. Acid. Res. Mol. Biol. 63*, 39−67.
4. Wickner, S., and Hurwitz, J. (1974) *Proc. Natl. Acad. Sci. U.S.A. 71*, 4120−4124.
5. McMacken, R., Ueda, K., and Kornberg, A. (1977) *Proc. Natl. Acad. Sci. U.S.A. 74*, 4190−4194.
6. Wickner, S., and Hurwitz, J. (1975) *Proc. Natl. Acad. Sci. U.S.A. 72*, 3342−3346.
7. Shlomai, J., and Kornberg, A. (1980) *J. Biol. Chem. 255*, 6794−6798.
8. Zipursky, S. L., and Marians, K. J. (1980) *Proc. Natl. Acad. Sci. U.S.A. 77*, 6521−6525.
9. Shlomai, J., and Kornberg, A. (1980) *J. Biol. Chem. 255*, 6789−6793.
10. Marians, K. J. (1982) *J. Biol. Chem. 257*, 5656−5662.
11. Lee, M. S., and Marians, K. J. (1987) *Proc. Natl. Acad. Sci. U.S.A. 84*, 8345−8349.
12. Lasken, R., and Kornberg, A. (1988) *J. Biol Chem. 263*, 5512−5518.
13. Nurse, P., DiGate, R. J., Zavitz, K. H., and Marians, K. J. (1990) *Proc. Natl. Acad. Sci. U.S.A. 87*, 4615−4619.
14. Lee, E., H., Masai, H., Allen, G. C., Jr., and Kornberg, A. (1990) *Proc. Natl. Acad. Sci. U.S.A. 87*, 4620−4624.
15. McGlynn, P., Al-Deib, A. A., Liu, J., Marians, K. J., and Lloyd, R., G. (1997) *J. Mol. Biol. 270*, 212−221.
16. Nurse, P., Liu, J., and Marians, K. J. (1999) *J. Biol. Chem. 274*, 25026−25032.
17. Lohman, T. M., and Bjornson, K. P. (1996) *Annu. Rev. Biochem. 65*, 169−214.
18. Matson, S. W., and Kaiser-Rogers, K. A. (1990) *Annu. Rev. Biochem. 59*, 289−329.
19. Bujalowski, W., and Jezewska, M. J. (1995) *Biochemistry 34*, 8513−8519.
20. Jezewska, M. J., and Bujalowski, W. (1996) *Biochemistry 35*, 2117−2128.
21. Edeldoch, H. (1967) *Biochemistry 6*, 1948−1954.
22. Gill, S. C., and von Hippel, P. H. (1989) *Anal. Biochem. 182*, 319−326.
23. Bujalowski, W., Klonowska, M. M., and Jezewska, M. J. (1994) *J. Biol. Chem. 269*, 31350−31358.
24. Bujalowski, W., and Klonowska, M. M. (1994) *J. Biol. Chem. 269*, 31359−31371.
25. Bujalowski, W., and Klonowska, M. M. (1994) *Biochemistry 33*, 4682−4694.
26. Bujalowski, W., and Klonowska, M. M. (1993) *Biochemistry 32*, 5888−5900.
27. Secrist, J. A., Bario, J. R., Leonard, N. J., and Weber, G. (1972) *Biochemistry 11*, 3499−3506.
28. Ledneva, R. K., Razjivin, A. P., Kost, A. A., and Bogdanov, A. A. (1977) *Nucleic Acid Res. 5*, 4226−4243.
29. Jezewska, M. J., Rajendran, S., and Bujalowski, W. (1997) *Biochemistry 36*, 10320−10326.
30. Jezewska, M. J., Rajendran, S., and Bujalowski, W. (1998) *Biochemistry 37*, 3116−3136.
31. Jezewska, M. J., Rajendran S., and Bujalowski, W. (1998) *J. Biol. Chem. 273*, 9058−9069.
32. Jezewska, M. J., Rajendran S., Bujalowska, D., and Bujalowski, W. (1998) *J. Biol. Chem. 273*, 10515−10529.
33. Lakowicz, J. R. (1999) *Principle of Fluorescence Spectroscopy*, Plenum Press, New York.
34. Jezewska, M. J., Kim, U.-S., and Bujalowski, W. (1996) *Biochemistry 36*, 2129−2145.
35. Jezewska, M. J., and Bujalowski, W. (1997) *Biophys. Chem. 64*, 253−269.
36. Tolman, G. L., Barrio, J. R., and Leonard, N. J. (1974) *Biochemistry*, *13*, 4869−4878.
37. Baker, B. M., Vanderkooi, J., and Kallenbach, N. R. (1978) *Biopolymers 17*, 1361−1372.
38. Bujalowski, W., Lohman, T. M., and Anderson, C. F. (1989) *Biopolymers 28*, 1637−1643.
39. Epstein, I. R. (1978) *Biophys. Chem. 8*, 327−339.
40. McGhee, J. D., and von Hippel, P. H. (1974) *J. Mol. Biol. 86*, 469−489.
41. Hill, T. L. (1985) *Cooperativity Theory in Biochemistry*, Springer-Verlag, New York.
42. Record, M. T., Jr., Anderson, C. F., and Lohman, T. M. (1978) *Q. Rev. Biophys. 11*, 103−178.
43. Record, M. T., Lohman, T. M., and deHaseth, P. L. (1976) *J. Mol. Biol. 107*, 145−158.
44. Olmsted, M. C., Bond, J. P., Anderson, C. F., and Record, M. T. (1995) *Biophys. J. 68*, 634−647.

45. Von Hippel, P. H., and Schleich T. (1969) *Structure of Biological Macromolecules* (Timasheff, S., and Fasman, G. D., Eds.) Chapter 6, M. Dekker, New York.
46. Wong, I., Moore, K. J., Bjornson, K. J., Hsieh, J., and Lohman, T. M. (1996) *Biochemistry 35*, 5726−5734.
47. Dong, F., Gogol, E. P., and von Hippel, P. H. (1995) *J. Biol. Chem. 270*, 7462−7473.
48. Hingorani, M. M., and Patel, S. S. (1993) Biochemistry *32*, 12478−12487.
49. Jezewska, M. J., and Bujalowski, W. (1996) *J. Biol. Chem. 271*, 4261−4265.
50. Bujalowski, W., and Jezewska, M. J. (2000) *J. Mol. Biol. 295*, 831−852.
51. Bujalowski, W., and Jezewska, M. J. (2000) *Biochemistry 39*, 2106−2122.

BI001113Y